Feng Ellias Yuming (Orcid ID: 0000-0002-2781-9003)
Su Bei (Orcid ID: 0000-0002-1663-6295)
Oschlies Andreas (Orcid ID: 0000-0002-8295-4013)

Geoengineered ocean vertical water exchange can accelerate global deoxygenation

Ellias Yuming Feng[1,*], Bei Su[2,^], and Andreas Oschlies[1]

[1] GEOMAR Helmholtz Centre for Ocean Research Kiel, Germany.

[2] School of Environmental Sciences, University of Liverpool, United Kingdom.

[*] Current affiliation: Innoventure GmbH, Hamburg, Germany.

[^] Current affiliation: Institute of Marine Science and Technology, Shandong University, P. R. China.

Corresponding author: Andreas Oschlies (aoschlies@geomar.de)

Key Points:

- Artificial downwelling (AD) and upwelling (AU) in the eastern Pacific oxygen deficient region is simulated in a global model
- Both technologies can effectively mitigate local expansion of intermediate-depth oceanic oxygen deficient zones under climate change
- Global deoxygenation is however enhanced due to increased export production and aerobic respiration resulting from AD and AU

This article has been accepted for publication and undergone full peer review but has not been through the copyediting, typesetting, pagination and proofreading process which may lead to differences between this version and the Version of Record. Please cite this article as doi: 10.1029/2020GL088263

Abstract

Ocean deoxygenation is a threat to marine ecosystems. We evaluated the potential of two ocean intervention technologies, i.e. "artificial downwelling (AD)" and "artificial upwelling (AU)", for remedying the expansion of Oxygen Deficient Zones (ODZs). The model-based assessment simulated AD and AU implementations for 80 years along the eastern Pacific ODZ. When AD was simulated by pumping surface seawater to the 178 ~ 457 m depth range of the ODZ, vertically integrated oxygen increased by up to 4.5% in the deployment region. Pumping water from 457 m depth to the surface (i.e. AU), where it can equilibrate with the atmosphere, increased the vertically integrated oxygen by 1.03%. However, both simulated AD and AU increased biological production via enhanced nutrient supply to the sea surface, resulting in enhanced export production and subsequent aerobic remineralization also outside of the actual implementation region, and an ultimate net decline of global oceanic oxygen.

1 Introduction

In the ocean, oxygen is biologically produced through photosynthesis and consumed through the respiration and remineralization of organic matter. In addition to biological oxygen sources and sinks in the sea, oxygen is also supplied via air-sea gas exchange from the atmosphere. This supply is, however, predicted to become inhibited under global warming because of reduced oxygen solubility and strengthened ocean stratification (Keeling et al., 2010). A manifestation of the resulting ocean deoxygenation is the expansion of Oxygen Deficient Zones (ODZs) e.g. in the eastern tropical Pacific as demonstrated by more than 50 years of oxygen measurements (Stramma et al., 2008). Oxygen depletion will intensify marine hypoxia that can harm local ecosystems with possibly severe socio-economic impacts (Breitburg et al., 2018).

Although the ultimate solution to stop ocean deoxygenation is to stop greenhouse gas emissions, this is difficult to achieve promptly because of continued population growth associated with conflicting interests of individuals, societal and geopolitical actors (Raftery et al., 2017). In parallel to international efforts for mitigating climate change, measures to counter marine hypoxia have been tested with some success in a few coastal environments. One notable case of its kind is a 2.5-year-long experiment employing artificial downwelling (AD) to oxygenate the anoxic deep water at the By Fjord in southwestern Sweden (Stigebrandt et al., 2014). In their test, oxygen-rich surface water was pumped into the deep anoxic bottom waters (40 m depth) via vertical pipes, and dissolved oxygen concentrations of the previously anoxic bottom waters were stabilized at 60 to 180 μmol L^{-1} with no anoxia being observed during operation of the AD devices. AD might thus be considered as a possibly effective tool to oxygenate ODZs so that the expansion of marine dead zones could be mitigated or even stopped.

However, at least two concerns prevent us from conducting an *in situ* investigation like the By Fjord case in open-ocean ODZs: (*i*) The volume of global open-ocean ODZs (more than 2 x 10^{14} km^3, Ulloa et al., 2012) is much larger than the By Fjord and based on a previous example of pumping deep water into surface ocean (White et al., 2010), some key technical constraints such as structural robustness still remain major challenges; (*ii*) even if AD *in situ* experiments were technically feasible, perturbations triggered by AD deployment might cause serious and possibly irreversible harm to marine ecosystems in the ODZ systems, for which the environmental controls are still not fully understood (Oschlies et al., 2017). In particular, an observable oxygen enrichment via AD that suffices to decelerate the ODZ expansion would require intensive AD and associated water relocation to be implemented over large areas with likely risks to the marine environment.

In respect to the first concern, the history of artificial upwelling (AU), a previously proposed marine geoengineering technology (Lovelock & Rapley, 2007), indicates that developing technologically feasible AD devices to remedy ODZ expansions might be possible. AU was initially proposed for enhancing phytoplankton production and subsequent fish yield as it could supply nutrients to the surface mixed layer by artificially pumping up deeper nutrient-rich waters. With continued technical development of AU devices during the past decades, the currently discussed wave-driven AU prototypes could lift water from several hundred meters depth effectively at rates up to 50 $m^3 s^{-1}$ (Kirke, 2003). Since AU and AD are mostly similar in respect to their hardware design (e.g. pipelines and power sources) with the only apparent difference being the direction of flow, it is reasonable to assume that AD could be technically improved to allow oxygenation of open-ocean ODZs in the near future. Regarding the second concern, using numerical models to assess the environmental impacts of any large-scaled marine engineering has been a common approach in geoengineering research because it avoids direct intervention with the real marine environment. The results of numerical simulations of AU helped to improve our understanding of its limited potential in enhancing marine carbon uptake (Oschlies et al., 2010; Keller et al., 2014). Inspired by previous AU modelling studies, we here employ a numerical model for a first evaluation of the oxygenation potential as well as environmental side effects for an assumed deployment of AU and AD devices in the eastern tropical Pacific ODZ region. The current study leaves aside any discussions of engineering and legal implications of potential AD or AU implementation.

2 Materials and Methods

The model employed in this study is the University of Victoria Earth System Climate Model (UVic_ESCM) version 2.9 (Keller et al., 2012), which has been used for a series of modelling assessments of large-scale AU implementations (Keller et al., 2014; Oschlies et al., 2010). UVic consists of an energy-moisture equation-governed atmosphere, a terrestrial vegetation component based on TRIFFID (Top-down representation of interactive foliage and flora including dynamics), and a 3D ocean consisting of (*i*) MOM (Modular Ocean Model) for the ocean circulation, (*ii*) CO2sys for marine inorganic carbon chemistry (Lewis & Wallace, 1998), and, (*iii*) a NPZD (i.e. nutrient, phytoplankton, zooplankton and detritus)-oriented module for marine biogeochemistry (Keller et al., 2012). The marine NPZD module describes the growth (fertilized by nitrate and phosphate), mortality, and zooplankton predation of both nitrogen-fixing (diazotrophs) and non-fixing phytoplankton, while oxygen as a prognostic tracer is "generated" through phytoplankton photosynthesis and "consumed" through aerobic respiration (remineralization) of phytoplankton, zooplankton, and detritus. All UVic components share the same spatial resolution of 1.8 ° latitude x 3.6 ° longitude.

In our idealized model simulations, AD was assumed to be uniformly deployed as vertical pipes covering all coastal grid boxes of the eastern tropical Pacific ODZ between 15.3° N and 15.3° S (Figure 1a, area size 1.5 x 10^6 km^2). Currently proposed/tested pumping rates vary from 0.01 $m^3 s^{-1}$ (White et al., 2010) to 50 $m^3 s^{-1}$ (Kirke, 2003), which are usually constrained by different pipe geometries and power systems. Since the UVic model does not resolve the sub-grid hydrology below its resolution, operating AD at a rate of 1 $m^3 s^{-1}$ and a geographic density of 1 device per km^2 is equivalent to operating it at a rate of 0.01 $m^3 s^{-1}$ and a density of 100 devices per km^2, which are both equal to a modelled vertical flow of 1.5 Sv over the selected area (see Figure S1 for tests on different flow rates). Therefore, we omit the detailed characterization of the pipe system and use flow units (Sv) to represent the assigned artificial upwelling intensity. We prepared three sets of AD implementation strategies for a continuous operation from year 2020 to 2099 under the business-as-usual GHG emission

forcing outlined by the Representative Concentration Pathway 8.5 scenario (Meinshausen et al., 2011). The first AD run (name: *Deep_Downwelling*) as a benchmark, was assumed to generate constant downwelling at 1.5 Sv from the sea surface (upper end of the pipe) to 457 m (the fifth ocean layer of UVic), while a similar run (name: *Shallow_Downwelling*) with pipe length of 178 m (reaching the third ocean layer of UVic) was introduced to test how pipe depth can affect the environmental impacts. In the third AD model run (name: *Stabilization_Downwelling*), sea surface water was pumped to the same depth of *Deep_Downwelling*, but only when local oxygen concentrations there were lower than in year 2020. For comparison we also prepared an AU experiment resembling *Deep_Downwelling* run, but with water flowing upward instead of downward within the pipes (name: *Deep_Upwelling*).

To ensure volume conservation at AD implementation regions, a compensating upwelling flow was introduced locally at all intermediate levels in the grid-box columns where AD was implemented for every time steps with AD turned on (Figure 1b). We also assumed that the engineered AD devices pumped water adiabatically without any property change from the sea surface into the deep layer, whereas the compensating AU flow "outside" of the AD pipes consecutively displaced waters and their tracer contents (e.g. heat and oxygen) upward into a shallower layer. A corresponding compensating downwelling flow was introduced in the AU run (Figure 1c). For ocean grid boxes where water was shallower than proposed length of AD (AU) pipes, water was pumped to (from) the deepest local grid box. A control run (named *Control*) without any implementation of AD or AU served as a reference.

3 Results and discussion

The control run simulated an increase in global mean surface air temperature by 2.72 °C from year 2020 to 2099, while global oceanic oxygen decreased by 3% (Table 1). With implementations of AD and AU, model runs *Shallow_Downwelling*, *Deep_Downwelling*, *Stabilization_Downwelling* and *Deep_Upwelling* simulated only small deviations (less than 4 ppm and less than 0.1^{o}C with respect to the baseline values in 2099) for global atmospheric CO_2 concentration and surface air temperature (Figure S2), implying that AD&AU designed at our proposed scale will not alter global climate at noticeable levels. These relatively minor effects on atmospheric CO_2 and somewhat more substantial effects on surface temperatures is consistent with earlier studies (Oschlies et al., 2010; Keller et al., 2014). As expected, AD and AU effectively enriched the oceanic oxygen at their deployment sites, as indicated by (*i*) reduced fractions of regional suboxic waters (oxygen concentration less than 5 μmol/L) from 24.08% (*Control*) to 18.48% (*Shallow_Downwelling*), 7.48% (*Deep_Downwelling*) and 23.00% (*Deep_Upwelling*) (Figure 1d); (*ii*) increases in regional vertically-integrated oxygen content by 1.14% (*Shallow_Downwelling*), 4.5% (*Deep_Downwelling*), and 1.14% (*Deep_Upwelling*), respectively (Figure 2a, volume-integrated oxygen content: 0.177, 0.183, 0.177 Pmol, respectively) compared to that of *Control* (Table 1). However, *Stabilization_Downwelling* as the only non-constant AD case caused only 0.72 Sv water to be downwelled, resulting in almost unchanged regional oxygen contents (volume-integrated oxygen 0.174 Pmol, 0.7% less than that of *Control*), despite of a volume reduction of regional suboxic water by 20.83%. Neither AD nor AU had substantial impacts on surface oxygen concentrations in the implementation sites due to the effective heat and air-sea gas exchange, while the effective oxygen enrichment varied with depth (Figure 1f): For AD runs, highest oxygen enrichment was simulated at the lower ends of the AD pipes where AD deposited oxygen-saturated surface waters at depths usually depleted in oxygen. The subsurface waters above the lower end of the AD pipes, however, experienced a slight

reduction in oxygen compared to control run because AD-induced compensating upwelling brought up oxygen-poorer waters from deeper layers that were not sufficiently oxygenated by either O_2 air-sea flux or high-oxygen AD water (Figure 1b). The peak of oxygen enrichment from AU was observed below the surface, because AU-induced compensating downwelling from the surface could bring oxygen-saturated water to subsurface levels (Figure 1b). In summary, both AU and AD seem to be effective in enhancing oxygen levels in regions where they are deployed, making them theoretically viable tools to mitigate the expansion of ODZs such as the one of the eastern tropical Pacific focused on in our simulations. However, such effectiveness is found to only last for about a decade if AD and AU are terminated, e.g. after 20, 40 or 60 years of operation (Figure S3).

Perhaps the most noticeable unintended consequence of employing AD&AU to oxygenate ODZs, was the enhanced oxygen depletion outside the AD&AU deployment regions, resulting in (*i*) a continued expansion of the global suboxic volume (Table 1, Figure 1d) and (*ii*) decreased global oceanic oxygen content (Table 1, Figure 2a) in the AD&AU runs. Albeit small in relative terms, the global increase in suboxic volume is systematic and we do not expect that this side effect can be avoided. The mechanism behind this unexpected finding is as follows: both AD and AU caused nutrient enhancement at the sea surface in the region of deployment, through either compensated or engineered upwelling (Figure 3a, 3b, 3c, 3d and S4). Therefore, large areas near the eastern Pacific upwelling zone experienced enhanced export production (Figure 3e, 3f, 3g and 3h) and subsequent increase in remineralization (Figure 3i, 3j, 3k and 3l). It is worth noting that the eastern Pacific upwelling zone itself (Figure S5) is well-known for its abundant surface nutrients (nitrate and phosphate), thus phytoplankton growth in this area is not limited by inorganic nutrients and will therefore not be boosted by a further AD&AU-induced increase in surface nutrients. As a result, the AD&AU deployment region, unlike the areas near it, showed a slightly decreased export production affected mostly by upwelling-induced surface cooling (Figure 4a, 4b, 4c and 4d).

On the larger regional scale, the spatial patterns of enhanced export production (Figure 3e, 3f, 3g, 3h) share some similarities with those of (*i*) air-sea oxygen flux (Figure 4i, 4j, 4k to 4l), and (*ii*) vertically integrated aerobic remineralization (Figure 3i, 3j, 3k to 3l). For the patterns of (*i*) air-sea oxygen flux, the enhancement of export production from the AU&AD runs revealed an increase in net community production that consequently released more oxygen from the ocean to the atmosphere. As for the eastern Pacific upwelling zone with no significant production increase, AU&AD-induced surface cooling (Figure 4a, 4b, 4c and 4d) increased the oceanic oxygen solubility, hence more oxygen could be taken up by the ocean from the atmosphere (Figure 2b). Globally, the change in oxygen air-sea flux explained about half of total oceanic oxygen loss from AD runs compared to control run (Figure 2a and 2b). For changes in (*ii*) aerobic ocean remineralization, increased oxygen supply into the ODZs led to a decline in regional denitrification (Figure 2f). If nothing else was changed, this would result in enhanced aerobic respiration at the expense of reduced anaerobic denitrification, thereby enhancing oxygen consumption in the ocean interior and partly offsetting the oxygenation effect. After accounting for feedbacks of altered nutrient levels, in particular on nitrogen fixation, this resulted in a cumulative net oceanic nitrate global gain of 0.091 Pmol NO_3 in the *Deep-Downwelling* run, corresponding to an additional interior-ocean oxygen sink of 0.12 Pmol O_2 over the course of the simulation (Oschlies et al., 2019), explaining approximately the other half of oceanic oxygen loss in this AD run.

We found the ocean interior (Figure 2d, 4e, 4f, 4g, and 4h) was warmed by both AD and AU, among which the *Deep_Downwelling* increased the interior Pacific Ocean temperatures by up to 0.5 °C e.g. along the Asian coasts and in the South Pacific. Because the

downwelled warm water was laterally dispersed below the thermocline, the heating signals could propagate over large ocean areas below the sea surface. Since aerobic respiration is positively related to ambient temperature (Keller et al., 2012), warming of subsurface waters via AD and AU strengthened aerobic respiration and hence accelerated oxygen consumption in this depth range. In summary, decreased global oceanic oxygen is attributed to (*i*) quickly outgassing of newly produced O_2 to the atmosphere, and (*ii*) enhanced remineralization at depth and increased replacement of anaerobic denitrification by aerobic respiration.

On a larger scale, oxygen-enriched water in our simulations accumulated and downwelled in the North Pacific following the pathways of the ocean circulation, making this area experience increased oxygen levels (Figure S6). Regionally, the sea surface received either engineered upwelling via AU pipes, or compensating upwelling around the AD pipes. The upwelled subsurface water carrying high dissolved inorganic carbon to the sea surface and reduced the regional and global uptake of CO_2 from the atmosphere (Table 1 and Figure 2b).

Regarding the differences between AU and AD, AU reduced local export production and remineralization while AD increased both (crosses in Figure 2e). This can to a large extent be explained by regional sea surface temperatures being lowest in the AU run (regionally averaged SST was 27.09 °C for *Shallow_Downwelling*, 26.86 °C for *Deep_Downwelling*, 27.40 °C for *Stabilization_Downwelling* and 26.29 °C for *Deep_Upwelling*). Referenced to *Deep_Upwelling*, *Deep_Downwelling* displayed relatively high local surface nitrate by the end of year 2099 (Figure 2c). Such nitrate elevation was caused by compensating upwelling of subsurface waters (Figure 1b), which were elevated in nitrate concentrations resulting from reduced denitrification in response to the injection of oxygen into the ODZ (Figure. S7).

4 Conclusions

In our idealized model experiments, vertical water translocation such as AU and AD, could both enhance local oxygen levels, of which AD has particular advantage over AU as it could accurately increase oxygen concentration at targeted depths. Both AU and AD altered the ocean heat (cooling surface but warming interior), carbon (more CO_2 outgassing) and nitrogen cycles (altered denitrification and nitrogen fixation) in the deployment regions and beyond. In our simulations, both AU and AD increased nutrient supply to the surface ocean, and in consequence export production and subsequent aerobic remineralization. This led to a reduced global oceanic oxygen content and, somewhat counterintuitively, an expansion of oxygen deficient waters outside of the AD/AU deployment areas.

Implementation of AU or AD to mitigate the expansion of open-ocean ODZs would require large-scale deployment of AU/AD devices. As revealed by the non-local environmental side effects in this modeling study, such an effort would require very careful operation to avoid perturbing background stratification, as well as nitrogen and carbon cycles. We recommend that a more detailed assessment, in particular using regional high-resolution modelling, and a cautious management strategy are required before AU/AD could be considered as an effective tool to prevent ocean deoxygenation. Regarding the limitations of our study, the coarse resolution of the employed model prevents us from effectively investigating how pump density, pipe geometries and flow rates specifically affect the overall potential of AU/AD. It is also worth mentioning, that the involved environmental side effects, especially the profound increase in export production in the AD runs, was mostly related to our particular assumption of compensating upwelling, which was assumed to occur locally in the same grid box column as the deployed AD. Future work will have to test the AU/AD

implementation in fine-resolution ocean models to verify the results and assumptions employed in this study.

Acknowledgments and Data

We thank three anonymous reviewers for their very helpful comments in improving the manuscript. The authors acknowledge funding supports via the Cluster of Excellence "The Future Ocean" (CP1780), funded within the framework of the Excellence Initiative by the German Research Foundation (DFG), SFB 754 (Climate-Biogeochemistry interactions in the tropical oceans), and the Priority Program SPP 1689 (Climate Engineering – Risks, Challenges, Opportunities?). All authors declare that they have no potential conflicts of interests. Model outputs and other data used to produce the figures are uploaded to GEOMAR data server (**https://ftp3.geomar.de/users/yfeng/OxygenationAD/**). The authors appreciate the helpful discussions with colleagues from GEOMAR's Biogeochemical Modelling research group.

References

Breitburg, D., Levin, L. A., Oschlies, A., Grégoire, M., Chavez, F. P., Conley, D. J., et al. (2018). Declining oxygen in the global ocean and coastal waters. *Science*, *359*(6371), eaam7240.

Keeling, R. F., Körtzinger, A., & Gruber, N. (2010). Ocean deoxygenation in a warming world. *Annual Review of Marine Science*, *2*(1), 199–229.

Keller, D. P., Oschlies, A., & Eby, M. (2012). A new marine ecosystem model for the University of Victoria earth system climate model. *Geoscientific Model Development*, *5*(5), 1195–1220.

Keller, D. P., Feng, E. Y., & Oschlies, A. (2014). Potential climate engineering effectiveness and side effects during a high carbon dioxide-emission scenario. *Nature Communications*, *5*, 1–11.

Kirke, B. (2003). Enhancing fish stocks with wave-powered artificial upwelling. *Ocean and Coastal Management*, *46*(9–10), 901–915.

Lewis, E., & Wallace, D. W. R. (1998). Program developed for CO2 system calculations. Oak Ridge, TN, USA: Report ORNL/CDIAC-105 (Oak Ridge National Laboratory).

Lovelock, J. E., & Rapley, C. G. (2007). Ocean pipes could help the Earth to cure itself. *Nature*, *449*(7161), 403.

Meinshausen, M., Smith, S. J., Calvin, K., Daniel, J. S., Kainuma, M. L. T., Lamarque, J.-F., et al. (2011). The RCP greenhouse gas concentrations and their extensions from 1765 to 2300. *Climatic Change*, *109*(1–2), 213–241.

Oschlies, A., Pahlow, M., Yool, A., & Matear, R. J. (2010). Climate engineering by artificial ocean upwelling: Channelling the sorcerer's apprentice. Geophysical Research Letters, 37(4), L04701.

Oschlies, A., Duteil, O., Getzlaff, J., Koeve, W., Landolfi, A., & Schmidtko, S. (2017). Patterns of deoxygenation: Sensitivity to natural and anthropogenic drivers. Philosophical Transactions of the Royal Society A: Mathematical, Physical and Engineering Sciences, 375(2102). https://doi.org/10.1098/rsta.2016.0325

Oschlies, A., Koeve, W., Landolf, A., & Kähler, P. (2019). Loss of fixed nitrogen causes net oxygen gain in a warmer future ocean. *Nature Communications*, *10*(1), 1–7.

Raftery, A. E., Zimmer, A., Frierson, D. M. W., Startz, R., & Liu, P. (2017). Less than 2 °C warming by 2100 unlikely. *Nature Climate Change*, *7*(July).

Stigebrandt, A., Liljebladh, B., de Brabandere, L., Forth, M., Granmo, Å., Hall, P., et al. (2014). An experiment with forced oxygenation of the deepwater of the anoxic By

Fjord, Western Sweden. *Ambio*, *44*(1), 42–54.
Stramma, L., Johnson, G. C., Sprintall, J., & Mohrholz, V. (2008). Expanding Oxygen-Minimum Zones in the tropical oceans. *Science*, *320*(5876), 655 LP – 658.
Ulloa, O., Canfield, D. E., DeLong, E. F., Letelier, R. M., & Stewart, F. J. (2012). Microbial oceanography of anoxic oxygen minimum zones. *Proceedings of the National Academy of Sciences*, *109*(40), 15996 LP – 16003.
White, A., Björkman, K., Grabowski, E., Letelier, R., Poulos, S., Watkins, B., & Karl, D. (2010). An open ocean trial of controlled upwelling using wave pump technology. Journal of Atmospheric and Oceanic Technology, 27(2), 385–396. https://doi.org/10.1175/2009JTECHO679.1

Table 1. Model run setups and key outputs for control run

	Model run	Flow rate (Sv)	Pipe length (m)
AD&AU settings	*Shallow_Downwelling*	1.5	178
	Deep_Downwelling	1.5	457
	Deep_Upwelling	1.5	457
	Stabilization_Downwelling	0.72	457

Key outputs for control run[§]	Global				Regional			
	Year 2020	Year 2099	delta	delta (%)	Year 2020	Year 2099	delta	delta (%)
Atmospheric CO_2 concentration (ppm)	409.6	944.4	534.80	130.57	-	-		
Globally averaged atmospheric surface temperature (°C)	14.10	16.82	2.72	19.29	-	-		
Volume ratio of suboxic zones ¬ (%)	0.27	0.21	-0.06	22.22	21.25	24.08	2.83	13.32
Averaged sea surface temperature (°C)	18.46	20.30	1.84	9.97	25.85	27.87	2.02	7.81
Averaged ocean potential temperature*(°C)	6.40	7.21	0.81	12.66	7.07	7.87	0.80	11.32
Cumulative CO_2 input from air into the sea ^ (Pmol)	-	31.02			-	-0.17		
Cumulative O_2 input from air into the sea ^ (Pmol)	-	-7.84			-	0.14		
Averaged sea surface nitrate concentration (mmol m^{-3})	4.82	4.332	-0.49	-10.12	1.932	0.98	-0.95	-49.28
Averaged sea surface phosphate concentration (mmol m^{-3})	0.45	0.39	-0.06	-13.33	0.90	0.67	-0.23	-25.56
Arithmetically averaged sea surface pH	8.04	7.72	-0.32	-3.98	7.96	7.70	-0.26	-3.27
Volume-integrated oceanic oxygen content ^ (Pmol)	253.9	246.2	-7.7	-3.03	0.182	0.175	-0.007	-3.85
Cumulative change in ocean export production ^# (Pmol N)	-	6.41			-	0.066		
Cumulative change in interior ocean remineralization ^$ (Pmol N)	-	6.19			-	0.065		
Cumulative change in ocean denitrification ^ (Pmol N)	-	0.76			-	0.19		
Cumulative change in ocean nitrogen fixation ^ (Pmol N)	-	0.76			-	0.016		

§ From year 2020 to 2099, globally averaged and regionally averaged (AD and AU implementation areas) outputs are listed, followed by their differences in absolute changes and percentage changes to year 2020

¬ A ratio of the volume of suboxic ocean to that of entire ocean, calculated globally or regionally (restricted to only AD/AU implementation area)

* Values are averaged from 50 to 1600 m depth

^ Values are integrated from year 2020 to 2099

Only values from the first two ocean layers (0-130 m depth) are calculated, integrated from year 2020 to 2099

$ Only values below 130 m depth are integrated.

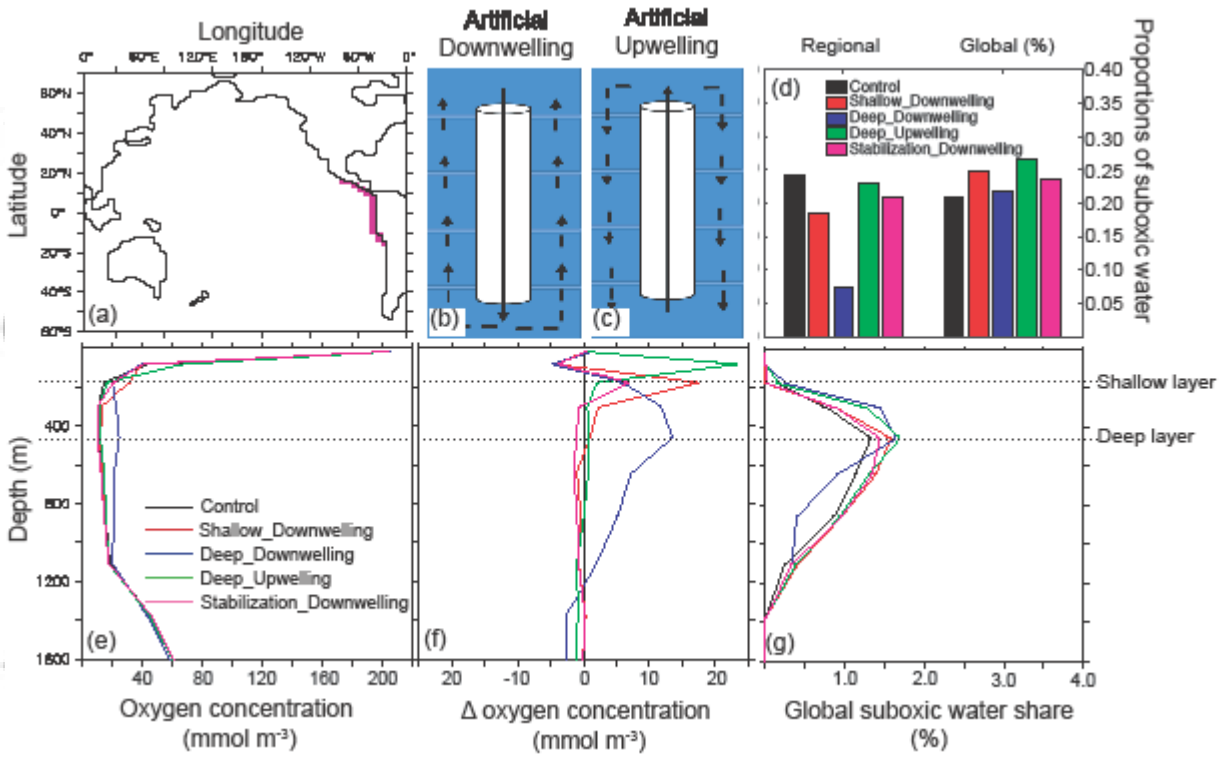

Figure 1. (a) Grid boxes along the west coast of Central and South America between 15.3° S and 15.3° N with AD (AU) implementation are marked violet (inside the dotted box). **(b, c)** Within each AD (AU) grid box, tracers were moved adiabatically from the sea surface layer to UVic's layer 3 (178 m depth) and 5 (457 m depth) for AD model run *Shallow_Downwelling* and *Deep_Downwelling*, respectively, while in the AU run (*Deep_Upwelling*) tracers were moved adiabatically from layer 5 to the sea surface, during which a compensating upwelling (downwelling) flow was initiated in each AD (AU) grid box column to conserve volume. **(d)** Simulated volume percentage fraction of suboxic waters (oxygen concentration less than 5 µmol/L) with respect to the global ocean, and volume fraction of regional suboxic waters with respect to the volume of the AD (AU) implementation area. **(e)** Vertical profile of area-averaged oxygen concentration in AD (AU) deployment regions. **(f)** Vertical profiles of AD (AU)-induced changes in oxygen concentration difference with respect to the control run in the deployment regions. **(g)** Vertical profile of the percentage of global suboxic area with respect to the global ocean area at the respective water depth. All results shown for model year 2099.

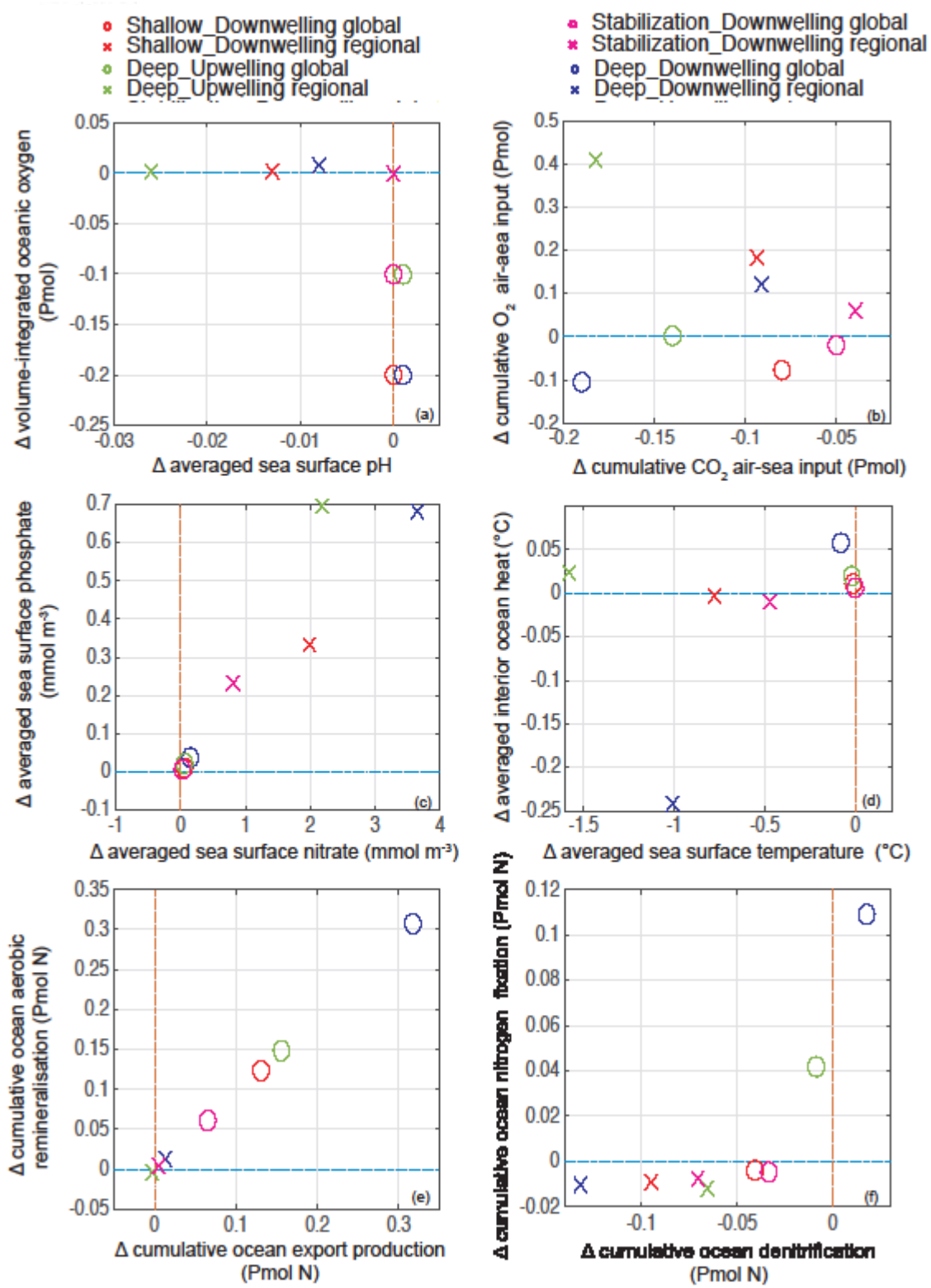

Figure 2. Differences between AD (AU) runs and the control run in year 2099. Globally averaged values are marked with circles while regionally (AD&AU implementation areas) averaged values are marked with crosses. The negative signs on panel (b)'s axes refer to a gas flux from sea to air. Cumulative aerobic remineralization in panel (e) is computed below a depth of 130 m, the same depth used to compute export production.

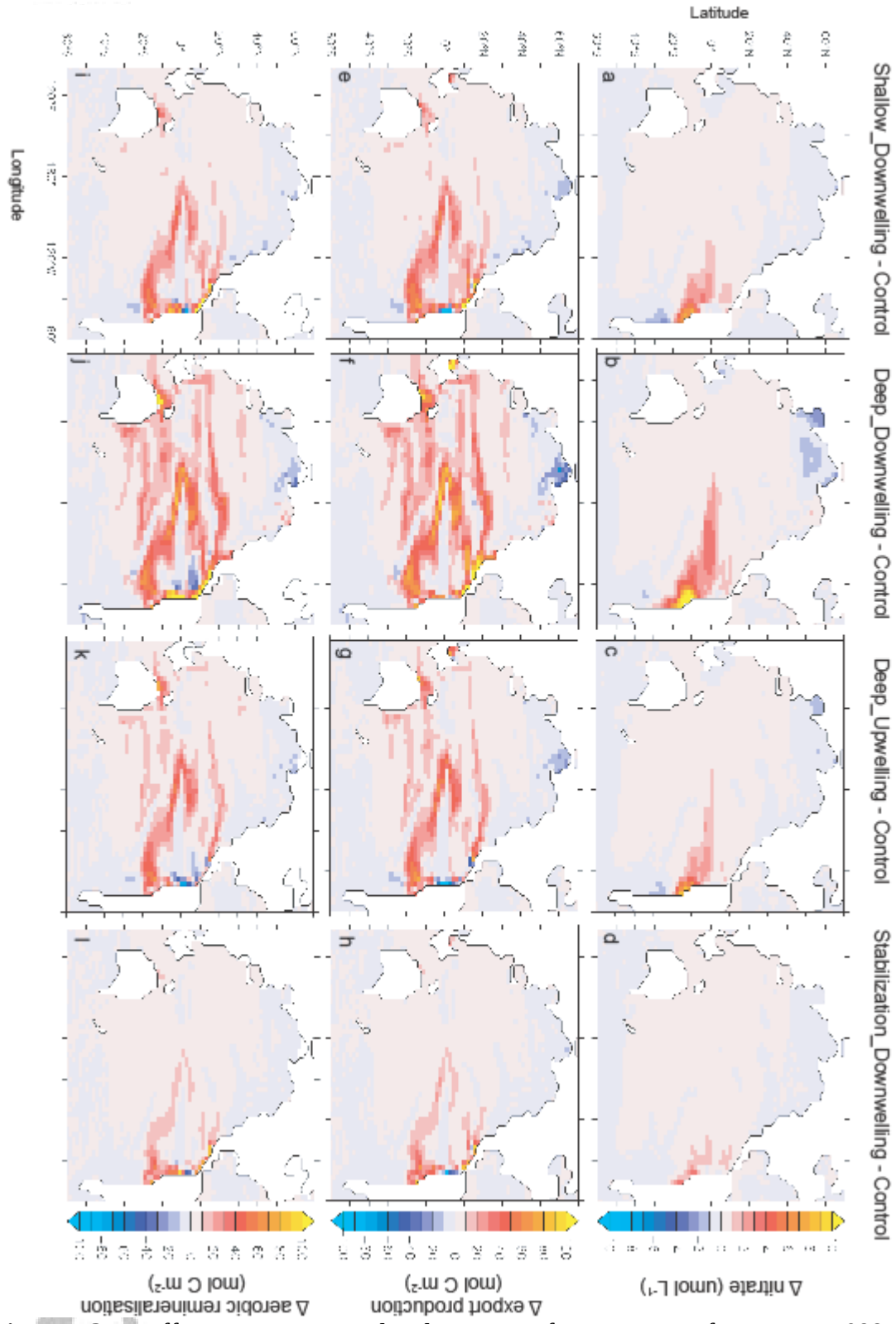

Figure 3. Differences in simulated sea surface nitrate for year 2099 of the *Shallow_Downwelling* (**a**), *Deep_Downwelling* (**b**), *Deep_Upwelling* (**c**), and *Stabilization_Downwelling* (**d**), respectively, with respect to the *Control* run; (**e**) (**f**) (**g**) (**h**) show the differences in cumulative (year 2020-2099) export production of the respective model runs; (**i**) (**j**) (**k**) (**l**) show the differences for cumulative aerobic remineralization.

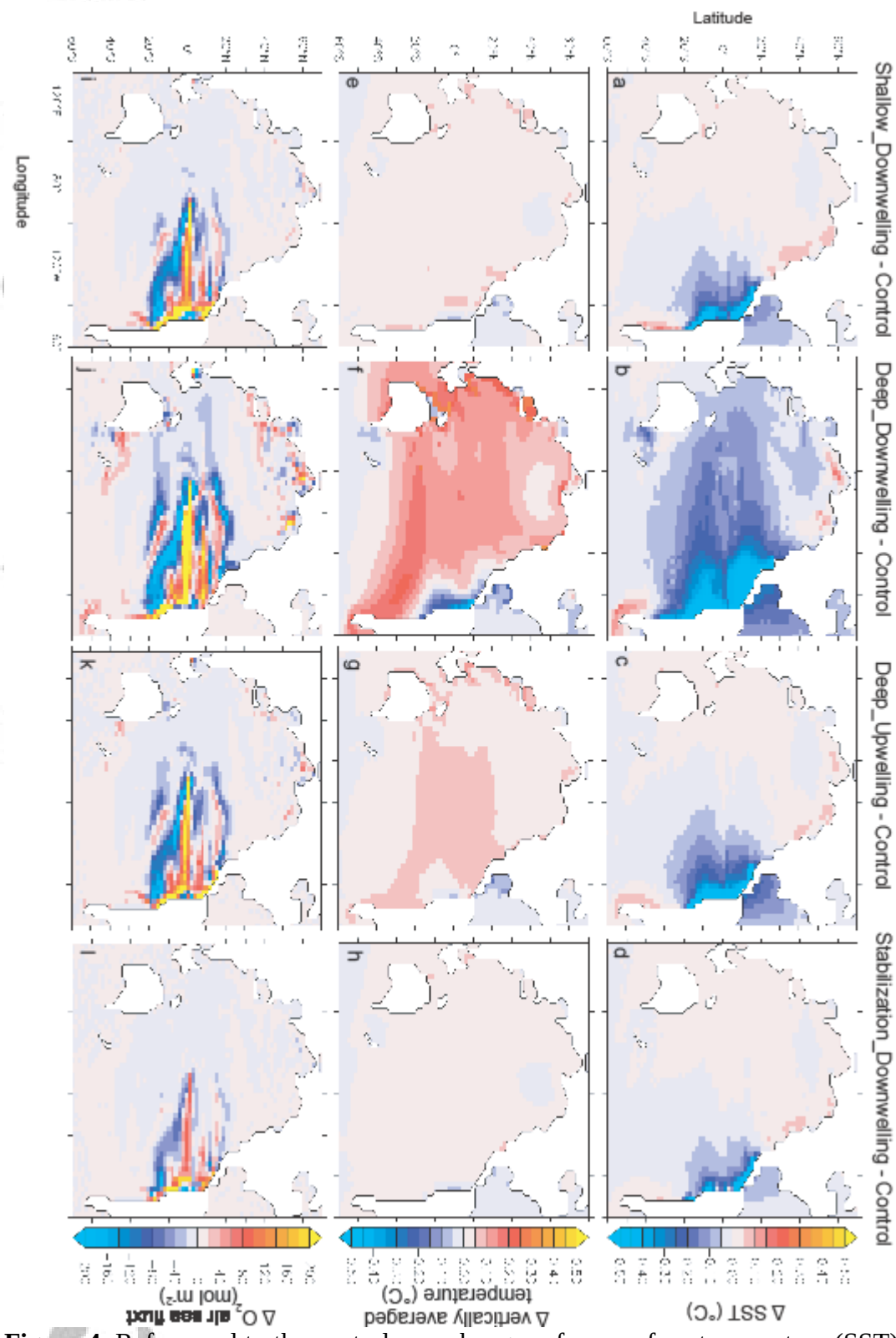

Figure 4. Referenced to the control run, changes of sea surface temperature (SST) simulated by run *Shallow_Downwelling* (**a**), *Deep_Downwelling* (**b**), *Deep_Upwelling* (**c**), and *Stabilization_Downwelling* (**d**), respectively, for year 2099; (**e**) (**f**) (**g**) (**h**) following the same order, corresponding changes in ocean temperature vertically averaged over 50-1600 m depth in year 2099; (**i**) (**j**) (**k**) (**l**) changes in cumulative O_2 air-sea fluxes (positive values indicate an oxygen flux into the ocean) from year 2020 to 2099.